8

Introduction to the Elastic Continuum Theory of Liquid Crystals

Ping Sheng

RCA Laboratories, Princeton, N. J. 08540

1. Introduction

In the preceding chapters of this book we have seen that in terms of molecular theories[1,2] one can calculate and successfully explain various properties of meosphase transitions. However, there exists a class of liquid-crystal phenomena involving the response of bulk liquid-crystal samples to external disturbances, with respect to which the usefulness of a molecular theory is not immediately obvious. These phenomena are usually distinguished by two characteristics: (1) the energy involved, per molecule, in producing these effects is small compared to the strength of intermolecular interaction; and (2) the characteristic distances involved in these phenomena are large compared to molecular dimensions. In describing these large-scale phenomena, it is more convenient to regard the liquid crystal as a continuous medium with a set of elastic constants than to treat it on a molecular basis. Based on this viewpoint, Zocher,[3] Oseen,[4] and Frank[5] devel-

oped a phenomenological continuum theory of liquid crystals that is very successful in explaining various magnetic (electric) field-induced effects. It is the purpose of the present chapter to develop this elastic continuum theory for nematic and cholesteric liquid crystals and to discuss and illustrate its use. In this paper, the derivation of the fundamental equation of the elastic continuum theory is followed by the application of the theory to four effects: (1) the twisted nematic cell, (2) the magnetic (electric) coherence length, (3) the Fréedericksz transition, and (4) the magnetic (electric) field-induced cholesteric–nematic transition.

2. The Fundamental Equation of the Continuum Theory of Liquid Crystals

In earlier chapters we have seen that liquid crystals are characterized by an orientational order of their constituent rod-like molecules.[1,2,6,7] In nematic liquid crystals this orientational order has uniaxial (cylindrical) symmetry, the axis of uniaxial symmetry being parallel to a unit vector $\hat{n}$, called the director. Let us now consider a very small spatial region inside a macroscopic sample of nematic liquid crystal that contains a sufficiently large number of molecules so that the long-range orientational order is well defined within that region. Such a spatial region can be characterized by a director pointing along the of local axis of uniaxial orientational symmetry. Let us imagine the division of the macroscopic sample into such small spatial regions. In each of the regions, we define an orientational director. In this manner the macroscopic sample of nematic liquid crystal can be characterized by a local director at every spatial "point," where we use the term point loosely to mean a small region of space as defined above. Obviously, this characterization of orientational order by a director field, $\hat{n}(\vec{r})$, is not limited to nematic liquid crystals, which we have used as an example in the above discussion. In fact, the director-field characterization can be applied equally well to cholesteric liquid crystals, since, locally, cholesterics also possess uniaxial symmetry in their orientational order. However, for convenience, we will continue to use nematic liquid crystals as our reference in the following discussion. The generalization of the theory will be made at appropriate places to permit application to cholesteric liquid crystals. In what follows, we first consider the free energy associated with a distortion in the director field. Next, we examine the free energy associated with the interaction of liquid crystals with external fields. The combination of all the free-energy contributions then yields the fundamental equation, which is an expression for the

total free energy of a sample of nematic or cholesteric liquid crystal in an external field.

The starting point for the development of continuum theory is the consideration of the equilibrium state. In nematic liquid crystals, parallel alignment of all the local directors represents the equilibrium state, or the state of minimum free energy. However, when we perturb the system by pinning the surface directors to the walls of the container, applying an external field, or introducing thermal fluctuations, the local directors will no longer be spatially invariant. A quantitative formulation of the above statements is that the quantities dn_α/dx_β, (where x is the spatial variable and the subscripts α,β = 1,2,3 denote the components along the three orthogonal axes of the Cartesian coordinate system) are zero for the equilibrium state but are nonzero for some, or all, values of α and β when the system is distorted. In other words, we can think of dn_α/dx_β as the distortion parameters, and the equilibrium state is given by the uniformly aligned state for which $dn_\alpha/dx_\beta = 0$ everywhere. Since the distorted state represents a state with higher free energy than the equilibrium state, we can write the free-energy density of the distorted state as

$$f(\text{distorted}) = f_0(\text{equilibrium}) + \Delta f, \qquad [1]$$

where f and f_0 are the free-energy densities of the distorted and equilibrium states, respectively; Δf (>0) is a function of the n_α and the dn_α/dx_β that vanishes when all $dn_\alpha/dx_\beta = 0$. Since, in general, $dn_\alpha/dx_\beta \ll (\text{molecular dimension})^{-1}$ for the phenomena of interest, we can expand Δf as a power series in the n_α and the dn_α/dx_β and retain only the lowest-order nonvanishing terms of the series. Let $\mathfrak{F}_D$ (subscript D stands for distortion) denote such an approximation to Δf. $\mathfrak{F}_D$ must satisfy several requirements. First, since we are expanding in powers of the dn_α/dx_β around $dn_\alpha/dx_\beta = 0$, which is a free-energy minimum, the lowest-order nonvanishing terms must be quadratic in the dn_α/dx_β (i.e. proportional to terms of the form $(dn_\alpha/dx_\beta)\cdot(dn_\gamma/dx_\delta)$). Second, since the "head" and the "tail" of a nematic director represent the same physical state, $\mathfrak{F}_D$ must be even in the n_α. Third, $\mathfrak{F}_D$ must be a scalar quantity. In addition, we will discard terms of the form $\nabla\cdot\vec{u}(\vec{r})$ where $\vec{u}(\vec{r})$ is any arbitrary vector field, since they represent surface contributions to the distortion free-energy density and are assumed to be small (by Gauss's Theorem, $\int\nabla\cdot\vec{u}(\vec{r})dV = \int d\hat{\sigma}\cdot\vec{u}(\vec{r})$, where $d\hat{\sigma}$ is a surface element with unit vector perpendicular to the surface). With the above constraints, it can be shown[5] that $\mathfrak{F}_D$ contains only three linearly independent terms. They are (1)

$[\nabla \cdot \hat{n}(\vec{r})]^2$, (2) $[\hat{n}(\vec{r}) \cdot \nabla \times \hat{n}(\vec{r})]^2$, and (3) $[\hat{n}(\vec{r}) \times \nabla \times \hat{n}(\vec{r})]^2$. It is obvious that all three terms satisfy the requirements stated above. Interested readers are referred to Refs. [5] and [8] for proofs that these three terms are indeed unique. In Fig. 1 we show the physical distor-

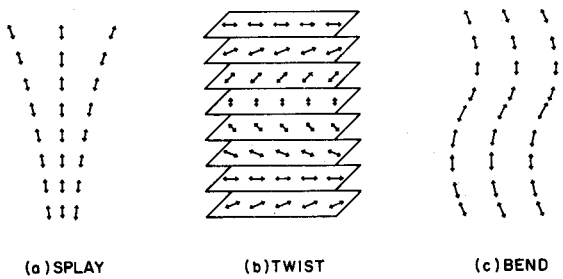

Fig. 1—Three types of distortion in a director field: (a) gives $\nabla \cdot \hat{n}(\vec{r}) \neq 0$, (b) gives $\hat{n}(\vec{r}) \cdot \nabla \times \hat{n}(\vec{r}) \neq 0$, and (c) gives $\hat{n}(\vec{r}) \times \nabla \times \hat{n}(\vec{r}) \neq 0$. Each director is shown with double arrows in order to indicate that the "head" and the "tail" directions represent exactly the same physical state in a nematic sample.

tions of the director field associated with the three terms. The first term is called "splay," the second term "twist," and the third term "bend." $\mathcal{F}_D$ can now be written as

$$\mathcal{F}_D = \frac{1}{2}\{K_{11}[\nabla \cdot \hat{n}(\vec{r})]^2 + K_{22}[\hat{n}(\vec{r}) \cdot \nabla \times \hat{n}(\vec{r})]^2 + K_{33}[\hat{n}(\vec{r}) \times \nabla \times \hat{n}(\vec{r})]^2\}, \quad [2]$$

where the constants K_{11}, K_{22}, K_{33} are, respectively, the splay, twist, and bend elastic constants and are named collectively as the Frank elastic constants. The factor $\frac{1}{2}$ is included so that the K's may agree with their historical definitions. Since $\mathcal{F}_D$ must be positive in order to give stability for the uniformly aligned state, all the K's must be positive. As for their values, we note that the theoretical determination of the K's from molecular parameters represents a task of linking the continuum theory to the microscopic theories of liquid crystals and is beyond the scope of the present paper. However, from dimensional analysis we can get an order-of-magnitude estimate of what the values of the K's should be. Since the K's are in units of energy/length, we must look for the characteristic energy and length in the problem. The only energy in the problem is the intermolecular inter-

action energy, which is estimated* to be ~0.01 eV, and the only suitable length is the separation between two molecules, which is ~10 Å. Therefore, $K \simeq 10^{-7}$ dyne, in order-of-magnitude agreement with measured values[8] of 10^{-7}–10^{-6} dyne. The K's are also temperature dependent. In fact, it can be shown[9] that the temperature dependence is of the form $K \sim <P_2(\cos\Theta)>^2$, where $< >$ denotes averaging over that small volume of the sample that is characterized by a local director $\hat{n}(\vec{r})$, P_2 is the Legendre polynomial of second order, and Θ is the angle between any molecule (inside the volume where the average is taken) and the local director $\hat{n}(\vec{r})$. $< P_2(\cos\Theta) >$ is just the local order parameter measured with $\hat{n}(\vec{r})$ as the axis of symmetry. The dependence of the K's on the square of the local order parameter is plausible if one thinks of the K's as the macroscopic analog of the anisotropic intermolecular interaction constants, the difference being that, in place of molecules, we have small volumes of the sample with well-defined long-range orientational order. In such an analogy $<P_2(\cos\Theta)>$ plays the role of a (temperature-dependent) dipole strength of the molecules.

Suppose now the sample of nematic liquid crystal is placed under the influence of a magnetic or an electric field. Because the liquid crystal molecules are generally diamagnetic, electrically polarizable, and anisotropic in their magnetic and electric properties, the application of a field usually contributes an amount of free-energy density which is opposite in sign to that of the distortion free-energy density (because fields help align molecules). Let us first discuss the magnetic field contribution. Consider again a small region of the sample characterized by a local director $\hat{n}(\vec{r})$. The diamagnetic susceptibility per unit volume in such a small volume is usually anisotropic. Let $\chi_\parallel$ denote the susceptibility per unit volume parallel to $\hat{n}(\vec{r})$ and $\chi_\perp$ denote the susceptibility per unit volume perpendicular to $\hat{n}(\vec{r})$. The difference, $\Delta\chi \equiv \chi_\parallel - \chi_\perp$, is a measure of the local anisotropy. As shown in Ref. [6], $\Delta\chi$ is equal to $N < P_2(\cos\Theta) > (\zeta_\parallel - \zeta_\perp)$, where N is the number of molecules per unit volume, $< P_2(\cos\Theta) >$ is the orientational order within the small region under consideration, and $\zeta_\parallel(\zeta_\perp)$ is the diamagnetic susceptibility of a single rod-like molecule

* The intermolecular interaction energy responsible for the nematic ordering can be estimated from the latent heat of isotropic–nematic phase transition $\Delta E \simeq 300$ cal/mol $\simeq 0.01$ eV/molecule (see, for example, G. H. Brown, J. W. Doane, and D. D. Neff, *A Review of the Structure and Physical Properties of Liquid Crystals,* p. 43, CRC Press, Cleveland, Ohio, 1971).

parallel (perpendicular) to its long axis. In the following we will assume that $\chi_{\parallel} > \chi_{\perp}$ (i.e., positive anisotropy) and that the value of $<P_2(\cos\,\Theta)>$ is uniform throughout the volume of the sample, implying that $\Delta\chi$, K_{11}, K_{22}, and K_{33} have no spatial dependence. In

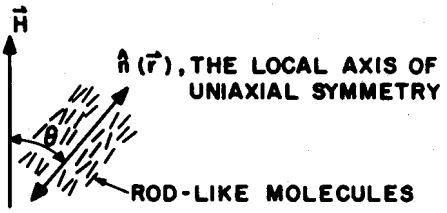

Fig. 2—Orientation of the local axis of uniaxial symmetry with respect to the external magnetic field direction.

Fig. 2 we show the relative directions of magnetic field $\vec{H}$ and local director $\hat{n}(\vec{r})$. The induced diamagnetic moments per unit volume parallel and perpendicular to $\hat{n}(\vec{r})$ are, respectively,

$$M_{\parallel} = H\chi_{\parallel}\cos\theta,$$
$$M_{\perp} = H\chi_{\perp}\sin\theta.$$

The work done by the field per unit volume is

$$W_{\text{magnetic}} = \int_0^H (-M_{\perp}'\sin\theta - M_{\parallel}'\cos\theta)\,dH'$$
$$= -\frac{H^2}{2}(\chi_{\perp} + \Delta\chi\cos^2\theta).$$

Discarding the spatially invariant term, $-H^2\chi_{\perp}/2$, we obtain the magnetic field contribution to the free-energy density

$$\mathcal{F}_M = -\frac{\Delta\chi}{2}[\vec{H}\cdot\hat{n}(\vec{r})]^2. \qquad [3]$$

Using similar arguments as above, we obtain the electric-field contribution to the free-energy density

$$\mathcal{F}_E = -\frac{\Delta\epsilon}{8\pi}[\vec{E}\cdot\hat{n}(\vec{r})]^2, \qquad [4]$$

where $\Delta\epsilon \equiv \epsilon_{\parallel} - \epsilon_{\perp}$ is the difference between the local dielectric con-

stants in directions parallel and perpendicular to the local director. Values of $\Delta\chi$ and $\Delta\epsilon$ typically range from 10^{-7}–10^{-6} cgs units for $\Delta\chi$ and 0.1–1 for $\Delta\epsilon$.

At this point we make a slight generalization so that the theory can be applied to cholesteric liquid crystals as well. The basic difference between cholesteric and nematic liquid crystals lies in the fact that the equilibrium state of cholesterics is characterized by a nonvanishing twist in the director field. If we denote the cholesteric helical axis as the x-axis, the equilibrium state is characterized by

$$\begin{aligned} n_x &= 0, \\ n_y &= \cos(\pi x/\lambda_0), \\ n_z &= \sin(\pi x/\lambda_0), \end{aligned}$$

where λ_0 is the pitch of the helix. Using this representation of the director field, the twist term, $[\hat{n}(\vec{r}) \cdot \nabla \times \hat{n}(\vec{r})]^2$, is calculated to be $(\pi/\lambda_0)^2$. This suggests that the twist part of free-energy density for the cholesteric liquid crystals should be expanded around $|\hat{n}(\vec{r}) \cdot \nabla \times \hat{n}(\vec{r})| = \pi/\lambda_0$, where $||$ is the absolute value sign. In fact, it can be shown[5] that the appropriate form is $[|\hat{n}(\vec{r}) \cdot \nabla \times \hat{n}(\vec{r})| - \pi/\lambda_0]^2$.

We are now in a position to combine all the free-energy density terms to give a total free-energy density $\mathcal{F}$ of the system under external fields:

$$\begin{aligned} \mathcal{F} &= \mathcal{F}_D + \mathcal{F}_M + \mathcal{F}_E \\ &= \frac{1}{2}\Big\{K_{11}[\nabla \cdot \hat{n}(\vec{r})]^2 + K_{22}\Big[\Big|\hat{n}(\vec{r}) \cdot \nabla \times \hat{n}(\vec{r})\Big| - \frac{\pi}{\lambda_0}\Big]^2 \\ &+ K_{33}[\hat{n}(\vec{r}) \times \nabla \times \hat{n}(\vec{r})]^2 - \Delta\chi[\vec{H} \cdot \hat{n}(\vec{r})]^2 - \frac{1}{4\pi}\Delta\epsilon[\vec{E} \cdot \hat{n}(\vec{r})]^2\Big\}. \end{aligned} \quad [5]$$

The total free energy of the sample is given by

$$F = \int_{\substack{\text{volume} \\ \text{of the sample}}} \mathcal{F}\, d^3r. \quad [6]$$

Eqs. [5] and [6] are the fundamental equations of the elastic continuum theory of nematic and cholesteric liquid crystals (for nematics λ_0 in Eq. [5] is set equal to ∞). In the following section we use the fundamental equations to solve four examples as illustrations for their applications.

3. Applications of the Elastic Continuum Theory

The basic principle involved in the application of the fundamental equations to the solution of actual problems is that the equilibrium state of the director field is always given by that director configuration that minimizes the free energy of the system with specified boundary conditions.

Before getting into actual calculations we first simplify Eq. [5] by setting $K_{11} = K_{22} = K_{33} = K$. This greatly facilitates the mathematics but does not affect the qualitative behavior of the results. Neglecting the term π/λ_0 for the moment, we have

$$\begin{aligned}\mathcal{F} &= \frac{K}{2}\Big\{[\nabla\cdot\hat{n}(\vec{r})]^2 + [\hat{n}(\vec{r})\cdot\nabla\times\hat{n}(\vec{r})]^2 + [\hat{n}(\vec{r})\times\nabla\times\hat{n}(\vec{r})]^2 \\ &\quad - \frac{\Delta\chi}{K}[\vec{H}\cdot\hat{n}(\vec{r})]^2 - \frac{1}{4\pi}\frac{\Delta\epsilon}{K}[\vec{E}\cdot\hat{n}(\vec{r})]^2\Big\} \\ &= \frac{K}{2}\Big\{[\nabla\cdot\hat{n}(\vec{r})]^2 + [\nabla\times\hat{n}(\vec{r})]^2 - \frac{\Delta\chi}{K}[\vec{H}\cdot\hat{n}(\vec{r})]^2 \\ &\quad - \frac{1}{4\pi}\frac{\Delta\epsilon}{K}[\vec{E}\cdot\hat{n}(\vec{r})]^2\Big\}. \end{aligned} \qquad [7]$$

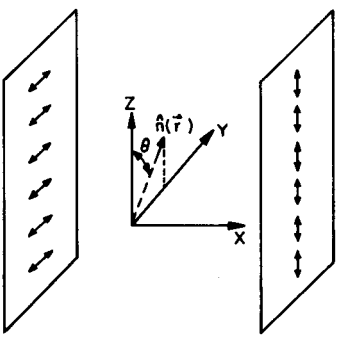

Fig. 3—The geometry of a 90°-twisted nematic cell.

3.1 Twisted Nematic Cell

In Fig. 3 we show a planar cell containing nematic liquid crystal, two of whose bounding walls are rubbed or otherwise treated so that the directors near the walls are pinned in the directions shown. Since the

directors at the two walls are perpendicular to each other, the local nematic directors must undergo a 90° twist in passing from one wall to the other. The question is how this twist is distributed across the cell, i.e., should the distribution be uniform or nonuniform? To answer this question, we must calculate the free energy of an arbitrary twist pattern with the specified boundary conditions. The correct twist pattern is then given by that director configuration that minimizes the free energy of the system. Assuming all the directors lie in the y-z plane, we write

$$n_x = 0,$$
$$n_y = \sin\theta(x),$$
$$n_z = \cos\theta(x).$$

From this representation of the director field, it is easily calculated that $\nabla \cdot \hat{n}(\vec{r}) = 0$ and $\nabla \times \hat{n}(\vec{r}) = (d\theta(x)/dx)[\sin\theta\hat{j} + \cos\theta\hat{k}]$, where we use $\hat{i},\hat{j},\hat{k}$ to denote the unit vectors in the x,y,z directions, respectively. Using Eqs. [6] and [7], we obtain

$$\begin{aligned} F &= \int d^3r \frac{K}{2}[\nabla \times \hat{n}(\vec{r})]^2 \\ &= \frac{K}{2}\int d^3r\left[\frac{d\theta(x)}{dx}\right]^2 \\ &= \frac{KA}{2}\int_{\substack{\text{thickness}\\ \text{of the cell}}} dx\left[\frac{d\theta(x)}{dx}\right]^2, \end{aligned} \qquad [8]$$

where A is the area of the cell in the y-z plane. To minimize F, we recall that if one wants to minimize the value of an integral

$$I = \int_a^b G\left(y(x), \frac{dy(x)}{dx}, x\right)dx$$

by varying the functional form of $y(x)$, the optimal function $y(x)$ must satisfy the equation

$$\frac{\partial G}{\partial y} - \frac{d}{dx}\frac{\partial G}{\partial\left(\frac{dy}{dx}\right)} = 0, \qquad [9]$$

which is called the Euler–Lagrange equation. In our present case θ corresponds to y, and $G = [d\theta(x)/dx]^2$; the application of Eq. [9]

yields $d^2\theta(x)/dx^2 = 0$, or $d\theta(x)/dx = C$, where C is an integration constant that can be determined by the boundary condition $C\times$ (cell thickness) $= \pm\pi/2$ ($+\pi/2$ is indistinguishable from $-\pi/2$ for nematics). This is the result we are looking for. It tells us that the twist will be uniformly distributed across the cell. However, because $d\theta/dx$ can be either + or −, the twist can be either left handed or right handed. In an actual 90°-twisted nematic cell, both senses of the twist are usually present, a fact that is indicated by the existence of visible disinclination lines separating regions of opposite senses of the twist.

3.2 Magnetic Coherence Length

The geometry of this problem is shown in Fig. 4. A semi-infinite sample of nematic liquid crystal with positive anisotropy is bound on one

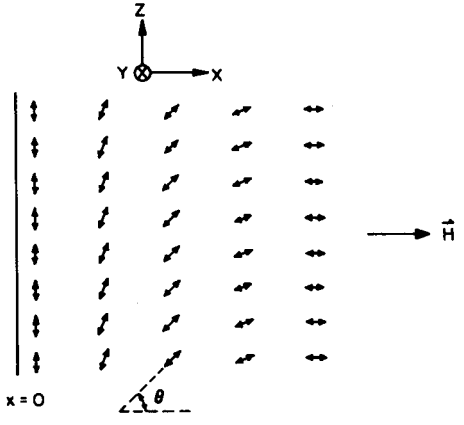

Fig. 4—Distortion of the director field when the molecules are pinned to the wall perpendicular to the external magnetic field direction. The nematic molecules are assumed to be diamagnetic with positive anisotropy.

side by a wall that is treated so that the directors near the wall are pinned along the z-direction. A magnetic field is applied along the x-axis, so that far away from the wall the directors would lie along the field direction. There is a transition region near the wall where the directors gradually change from one direction to the other. The problem is to find the characteristic length of that transition region. From

Fig. 4 we have

$$n_x = \cos\theta(x),$$
$$n_y = 0,$$
$$n_z = \sin\theta(x).$$

Straightforward calculation gives

$$[\nabla\cdot\hat{n}(\vec{r})]^2 = \sin^2\theta\left[\frac{d\theta(x)}{dx}\right]^2,$$
$$[\nabla \times \hat{n}(\vec{r})]^2 = \cos^2\theta\left[\frac{d\theta(x)}{dx}\right]^2,$$
$$-\frac{\Delta\chi}{K}[\vec{H}\cdot\hat{n}(\vec{r})]^2 = -\frac{\Delta\chi}{K}[H\cos\theta(x)]^2.$$

Substitution into Eq. [7] yields

$$\frac{F}{A} = \frac{K}{2}\int_0^\infty dx\left(\left[\frac{d\theta(x)}{dx}\right]^2 - \frac{\Delta\chi}{K}[H\cos\theta(x)]^2\right), \qquad [10]$$

where A is the area of the bounding wall. Application of the Euler–Lagrange equation to Eq. [10] gives an equation for the $\theta(x)$ that minimizes the free energy of the system:

$$\frac{K}{H^2\Delta\chi}\frac{d^2\theta(x)}{dx^2} - \sin\theta\cos\theta = 0. \qquad [11]$$

The combination $K/(H^2\Delta\chi)$ has the dimension of (length)^2. We define

$$\xi_M = \frac{1}{H}\sqrt{\frac{K}{\Delta\chi}} \qquad [12]$$

as the characteristic distance of the problem. Eq. [11] can now be rewritten as

$$\frac{\sin\theta\cos\theta}{\xi_M^2}\frac{d\theta}{dx} = \frac{d^2\theta}{dx^2}\frac{d\theta}{dx} = \frac{1}{2}\frac{d}{dx}\left(\frac{d\theta}{dx}\right)^2$$
$$\frac{\sin\theta}{\xi_M^2}\frac{d\sin\theta}{dx} = \frac{1}{2}\frac{d}{dx}\left(\frac{d\theta}{dx}\right)^2$$

or

$$\frac{1}{2}\frac{1}{\xi_M^2}\frac{d\sin^2\theta}{dx} = \frac{1}{2}\frac{d}{dx}\left(\frac{d\theta}{dx}\right)^2 \qquad [13]$$

Integration of Eq. [13] yields

$$\left(\frac{d\theta}{dx}\right)^2 = \left(\frac{\sin\theta}{\xi_M}\right)^2 + C.$$

The constant of integration is fixed by the condition that as $x \to \infty$, $\theta \to 0$ and $d\theta/dx \to 0$. Therefore $C = 0$, and

$$\frac{d\theta}{dx} = \pm \frac{\sin\theta}{\xi_M}.$$

Choosing the $-$ sign for $x > 0$ and integrating once more, we have

$$\ln\left(\tan\frac{\theta}{2}\right) = -\frac{x}{\xi_M},$$

or

$$\theta(x) = 2\arctan[\exp\{-x/\xi_M\}], \text{ where } x \geq 0. \qquad [14]$$

Eq. [14] is plotted in Fig. 5. As we can see, ξ_M is the characteristic length scale below which the magnetic field does not have much in-

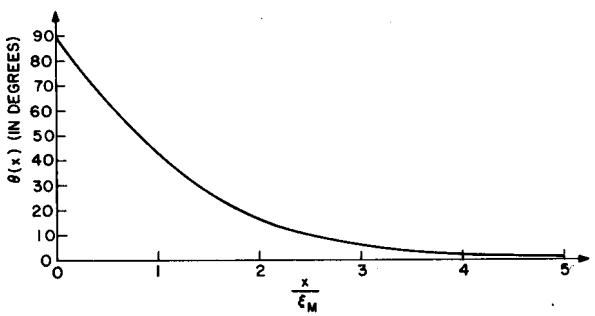

Fig. 5—Tilt angle (deviation from the field direction) of the director field plotted as a function of distance from the wall. The distance is measured in units of magnetic coherence length, which is the characteristic length of magnetic phenomena in nematic liquid crystals.

fluence on the relative orientations of the directors. Another way of saying the same thing is that ξ_M defines the scale of magnetic phenomena. ξ_M is usually called the "magnetic coherence length." For $K \sim 10^{-6}$ dyne, $\Delta\chi \sim 10^{-7}$ cgs units, and $H \sim 10$kOe, ξ_M is about 3 μm.

Suppose now that in place of the magnetic field an electric field is applied. If impurity conduction and other dynamical effects are neglected, the problem is qualitatively the same, and a quantity ξ_E can be obtained which is the exact analog of ξ_M. Substitution of $\Delta\epsilon/4\pi$ for $\Delta\chi$ and E for H in Eq. [12] gives

$$\xi_E \equiv \frac{1}{E}\sqrt{\frac{4\pi K}{\Delta\epsilon}}. \qquad [15]$$

Setting $\xi_M = \xi_E$, we can compare the relative effectiveness of magnetic and electric fields in orienting the nematic directors. The relation is

$$E = \sqrt{\frac{4\pi\Delta\chi}{\Delta\epsilon}}H. \qquad [16]$$

Taking $H = 1$ Oe, $\Delta\chi \sim 10^{-7}$ cgs unit, and $\Delta\epsilon \sim 0.1$, we have

$$E = \sqrt{\frac{4\pi\Delta\chi}{\Delta\epsilon}}H \simeq \sqrt{10^{-5}}H \simeq \frac{1}{300}\frac{\text{statvolt}}{\text{cm}} = 1 \text{ V/cm}.$$

Therefore, one oersted of magnetic field is equivalent to the order of one volt/cm of electric field in terms of effectiveness in orienting the nematic liquid crystals.

3.3 Fréedericksz Transition

Consider a planar cell of nematic liquid crystal with directors on both surfaces anchored perpendicular to the walls as shown in Fig. 6. It was first observed by Fréedericksz[10] in 1927 that such a cell would undergo an abrupt change in its optical properties when the strength of an external magnetic field, applied normal to the director (z-direction in Fig. 6), exceeded a well-defined threshold. (In the original experiment one wall of the cell was concave in shape so as to give some variation in the cell thickness.) Fréedericksz further noted that the strength of the magnetic field at threshold was inversely proportional to the cell thickness d.[11] This Fréedericksz transition is now a well-studied phenomenon, and has found applications in liquid-crystal display devices. The transition is essentially due to the magnetic alignment of the bulk sample directors at sufficiently high field strength. However, both the abruptness of its onset and the relationship between the threshold field strength and the cell thickness are of theoretical and practical interest. Here we will use the continuum

theory to calculate the various properties of the Fréedericksz transition. From Fig. 6 we get

$$n_x = \cos\theta(x),$$
$$n_y = 0,$$
$$n_z = \sin\theta(x).$$

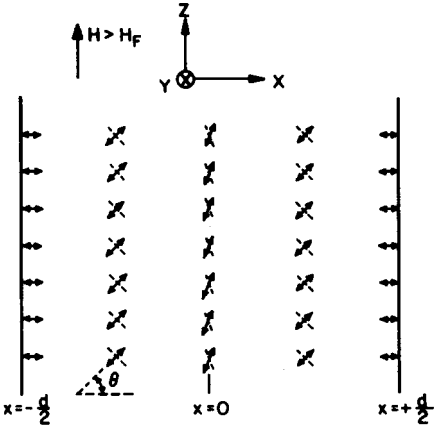

Fig. 6—Local nematic directors in a Fréedericksz cell when $H > H_F$. Dotted lines indicate the equivalent tilt configuration of the directors. Tilt angle θ is defined as shown.

From these expressions one obtains

$$[\nabla \cdot \hat{n}(\vec{r})]^2 + [\nabla \times \hat{n}(\vec{r})]^2 = \left[\frac{d\theta(x)}{dx}\right]^2,$$

and

$$-\frac{\Delta\chi}{K}[H \cdot \hat{n}(\vec{r})]^2 = -\frac{\Delta\chi}{K}H^2\sin^2\theta.$$

Substitution into Eq. [7] and application of the Euler–Lagrange equation results in

$$\xi_M{}^2 \frac{d^2\theta}{dx^2} + \sin\theta\cos\theta = 0. \qquad [17]$$

Using the same manipulations as those for Eq. [11], we get

$$\left(\frac{d\theta}{dx}\right)^2 = C - \frac{\sin^2\theta}{\xi_M{}^2}. \qquad [18]$$

The constant of integration C is obtained by noting that, from the symmetry of the problem, $d\theta/dx = 0$ at $x = 0$. Defining $\theta(x = 0)$ as θ_M, we get $C = \sin^2\theta_M/\xi_M{}^2$, and

$$\frac{d\theta}{dx} = \pm\frac{1}{\xi_M}\sqrt{\sin^2\theta_M - \sin^2\theta}, \qquad [19]$$

where the + sign corresponds to the solution in region $x < 0$ and the − sign corresponds to the solution in region $x > 0$. Since the solution is symmetric about $x = 0$, we will choose the + sign in the following calculations. Integration of Eq. [19] yields

$$\int_{-\frac{d}{2}}^{x} \frac{dx}{\xi_M} = \int_0^{\theta(x)} \frac{d\theta'}{\sqrt{\sin^2\theta_M - \sin^2\theta'}},$$

or

$$\frac{1}{\xi_M}\left(\frac{d}{2} + x\right)\sin\theta_M = \int_0^{\theta(x)} \frac{d\theta'}{\sqrt{1 - \left[\frac{\sin\theta'}{\sin\theta_M}\right]^2}}, \qquad [20]$$

where $-d/2 \leq x \leq 0$. The solution of Eq. [20] will proceed in two steps. First θ_M will be determined as a function of ξ_M (or of H, since $\xi_M \equiv \sqrt{K/\Delta\chi}/H$). Then this $\theta_M(H)$ can be substituted back into Eq. [20] for the solution of $\theta(x)$ as a function of H.

From the definition of θ_M we get

$$\frac{d}{2\xi_M}\sin\theta_M = \int_0^{\theta_M} \frac{d\theta'}{\sqrt{1 - \left(\frac{\sin\theta'}{\sin\theta_M}\right)^2}}. \qquad [21]$$

This equation can be solved graphically as in Fig. 7 by plotting, as a function of $\sin\theta_M$, the left- and right-hand sides on the same graph and locating the points of intersection. By expanding the integral on the right-hand side of Eq. [21], denoted here as $L(\sin\theta_M)$, for small values of θ_M, we get the slope

$$\left.\frac{dL(\sin\theta_M)}{d\,\sin\theta_M}\right|_{\theta_M = 0} = \frac{\pi}{2}.$$

Therefore, for $d/(2\xi_M) < \pi/2$ the only solution of Eq. [21] is $\theta_M = 0$.

However, when $d/(2\xi_M) > \pi/2$, a second solution with $\theta_M \neq 0$ is obtained that gives lower free energy than the $\theta_M = 0$ solution. The critical magnetic field H_F for the transition is found by equating $d/(2\xi_M)$

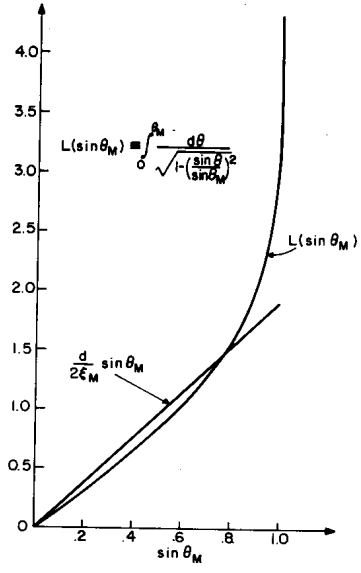

Fig. 7—Graphical solution of Eq. [21].

and $\pi/2$. Substitution of $\sqrt{K/\Delta\chi}/H$ for ξ_M gives

$$H_F = \sqrt{\frac{K}{\Delta\chi}}\frac{\pi}{d}, \qquad [22]$$

which agrees with Fréedericksz's observation that the threshold field strength varies inversely with the thickness of the sample. The form of Eq. [22] can be understood by a simple plausibility argument. In section 3.2 we have seen that the magnetic coherence length ξ_M can be thought of as that length below which the magnetic field does not have much influence on the relative orientations of the directors. By applying this interpretation of ξ_M to our present example it is clear that only when $\xi_M < d/2$ would it be possible for the magnetic field to have significant influence on the orientations of the directors. Therefore, we would estimate

$$H_F \simeq \sqrt{\frac{K}{\Delta\chi}}\frac{2}{d},$$

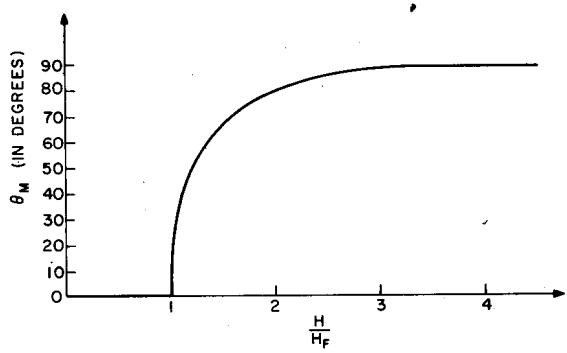

Fig. 8—Tilt angle of the directors at the center of Fréedericksz cell, θ_M, plotted as a function of reduced field H/H_F. For H/H_F slightly greater than 1, θ_M behaves as $\sim(H/H_F - 1)^{1/2}$.

which differs with the exact result only by a factor of $\pi/2$. In Fig. 8, θ_M is plotted as a function of H/H_F. For $H \sim H_F$, Eq. [21] can be expanded around $\theta_M = 0$ to give $\theta_M \propto (H - H_F)^{1/2}$.

Having obtained $\theta_M(H)$, we can now determine $\theta(x)$ as a function of H. By writing $d/2\xi_M = \pi H/2H_F$, Eq. [20] is put in the form

$$\frac{\pi}{2}\frac{H}{H_F}\left(1 + \frac{2x}{d}\right)\sin\theta_M = \int_0^{\theta(x)} \frac{d\theta'}{\sqrt{1 - \left(\frac{\sin\theta'}{\sin\theta_M}\right)^2}}. \qquad [23]$$

The right-hand side can be numerically integrated on computer, and the results $\theta(x)$ are plotted in Fig. 9 for three different values of H.

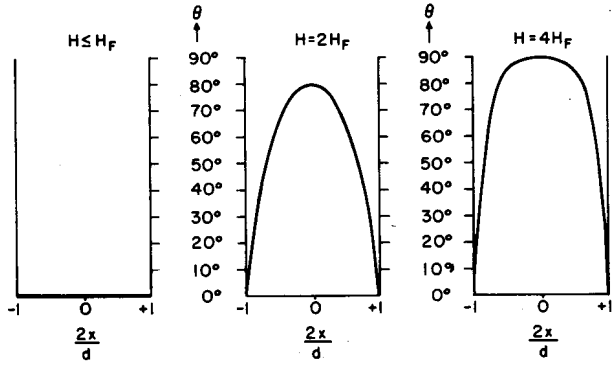

Fig. 9—Tilt angle of the directors plotted as a function of position in a Fréedericksz cell for three different magnetic field strengths.

The Fréedericksz transition can be induced by an electric field as well as by a magnetic field. The threshold electric field in that case is given by

$$E_F = \frac{\pi}{d}\sqrt{\frac{4\pi K}{\Delta\epsilon}}, \qquad [24]$$

or

$$V_F = E_F d = \pi\sqrt{\frac{4\pi K}{\Delta\epsilon}}. \qquad [25]$$

For $K \sim 10^{-6}$ dyne, $\Delta\chi \sim 10^{-7}$ cgs unit, $\Delta\epsilon \sim 0.1$, the critical magnetic field H_F is ~ 10 Oe for $d \sim 1$ cm, and the critical voltage is ~ 10 V, independent of cell thickness.

To conclude the discussion of the Fréedericksz transition, we note that for $H > H_F$ $(V > V_F)$ there are two equivalent tilt configurations of the directors, denoted by the solid and the dotted lines in Fig. 6. In practice, for $H > H_F$ (or $V > V_F$) both tilt configurations are usually present, and regions of different tilt patterns are separated by visible disinclination lines.

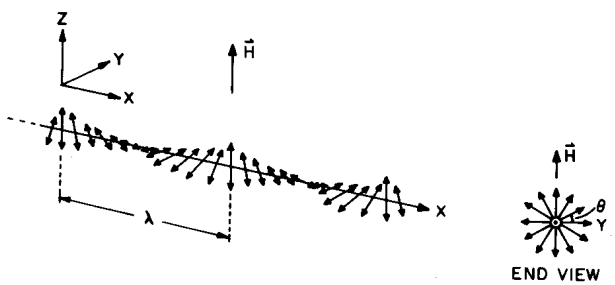

Fig. 10—Two views of the local directors in a cholesteric liquid crystal. In order to induce the cholesteric–nematic transition, a magnetic field H is applied perpendicular to the cholesteric helical axis. The angle θ used in the calculation is defined as shown.

3.4 Field-Induced Cholesteric–Nematic Transition

Consider a sample of cholesteric liquid crystal placed in a magnetic field H, with the field direction perpendicular to the cholesteric helical axis as shown in Fig. 10. From Eqs. [5], and [6], the free energy of the system over one period (or pitch) of the helix, λ, can be written as

$$\frac{F(\lambda)}{A} = \frac{K_{22}}{2}\int_0^{\lambda} dx \left\{ \left[\left| \hat{n}(\vec{r}) \cdot \nabla \times \hat{n}(\vec{r}) \right| - \frac{\pi}{\lambda_0} \right]^2 - \frac{\Delta\chi}{K_{22}} H^2 \sin^2\theta \right\}, \quad [26]$$

where A is the area of the sample in the y-z plane, assumed to be a constant, λ_0 is the pitch of the cholesteric helix at $H = 0$, θ is the angle between a local director and the y-axis as defined in Fig. 9,and $x = 0$ is defined by any point at which $\theta = 0$ (or π). With

$$n_x = 0,$$
$$n_y = \cos\theta(x),$$
$$n_z = \sin\theta(x),$$

we have

$$\hat{n}(\vec{r}) \cdot \nabla \times \hat{n}(\vec{r}) = \frac{d\theta(x)}{dx}$$

and

$$\frac{F(\lambda)}{A} = \frac{K_{22}}{2}\int_0^{\lambda} dx \left\{ \left[\frac{d\theta}{dx} - \frac{\pi}{\lambda_0} \right]^2 - \frac{\Delta\chi H^2 \sin^2\theta}{K_{22}} \right\}. \quad [27]$$

Here, we have to remember to take the absolute value of $d\theta/dx$. Application of the Euler–Lagrange equation yields

$$\xi_M{}^2 \frac{d^2\theta}{dx^2} + \sin\theta\cos\theta = 0,$$

which, as seen previously, can be put in the form

$$\left(\frac{d\theta}{dx}\right)^2 = \frac{1}{\xi_M{}^2}\left(\frac{1}{k^2} - \sin^2\theta\right), \quad [28]$$

where k^2 is an integration constant. At $H = 0$, it follows from Eq. [27] that $(d\theta/dx)$ equals a constant, (π/λ_0). Therefore, k must behave as $\sim H$ for $H \to 0$ in order to cancel the H^2 from $1/\xi_M{}^2$ in Eq. [28]. Writing Eq. [28] in the form

$$\frac{d\theta}{dx} = \pm\frac{1}{k\xi_M}\sqrt{1 - k^2\sin^2\theta}, \quad [28a]$$

we note that for finite values of H, $d\theta/dx$ is no longer a constant.

Plotting the z-component of the local director, $n_z = \sin\theta(x)$, as a function of position along the helical axis (x-axis) reveals that the sinusoidal pattern for $n_z(x)$ at $H = 0$ becomes distorted at finite values of H as shown in Fig. 11. The distortion makes $n_z(x)$ more square-wave-like and lengthens the pitch of the helix. Both of these effects can be understood on the basis that alignment along the magnetic

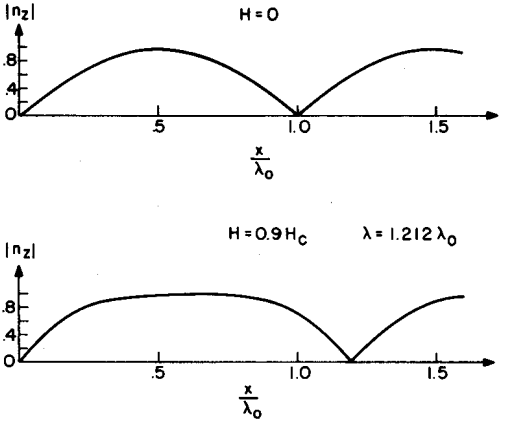

Fig. 11—Component of the cholesteric local director along the external field direction (z) for two different magnetic field strengths. Note that at finite field strength the helical pitch is lengthened and the sinusoidal shape of the curve at $H = 0$ is distorted, becoming more square-wave-like.

field direction lowers the energy of the system. The ± signs for $d\theta/dx$ indicate the two possible senses of the helical twist. Since they are equivalent, we choose the + sign in the following calculation. From the expression for $d\theta/dx$ we can get an expression for the pitch λ:

$$\lambda = \int_0^{\lambda} dx = \int_0^{\pi} d\theta \frac{dx}{d\theta} = \int_0^{\pi} \frac{\xi_M k}{\sqrt{1 - k^2 \sin^2\theta}} d\theta$$

$$= 2\xi_M k \int_0^{\frac{\pi}{2}} \frac{d\theta}{\sqrt{1 - k^2 \sin^2\theta}}. \qquad [29]$$

At this point, it becomes necessary to know k^2 as a function of H. To do that, we must substitute Eq. [28a] back into Eq. [27] and minimize the average free-energy density by varying k^2. Let us rewrite Eq. [27] as

$$g = \frac{2F(\lambda)}{q_0^2 K_{22} A\lambda} = \frac{1}{\lambda}\int_0^{\pi} d\theta \frac{dx}{d\theta}\left(\left[\frac{1}{q_0 \xi_M k}\sqrt{1 - k^2\sin^2\theta} - 1\right]^2 - \frac{\sin^2\theta}{q_0^2 \xi_M^2}\right), \quad [30]$$

where g is a dimensionless average free-energy density and $q_0 \equiv \pi/\lambda_0$. Substitution of Eq. [28a] for $dx/d\theta$ and expansion of the terms in the integrand gives

$$g = 1 - \frac{2\pi}{\lambda q_0} + \frac{2}{k\lambda \xi_M q_0^2}\int_0^{\pi} d\theta\sqrt{1 - k^2\sin^2\theta} - \frac{1}{k^2 q^2 \xi_M^2}. \quad [31]$$

Detailed steps leading from Eq. [30] to Eq. [31] are given in the Appendix. Differentiation of g with respect to k^2 yields

$$\frac{dg}{dk^2} = \frac{2\pi}{\lambda^2 q_0}\frac{d\lambda}{dk^2} - \frac{2}{k\lambda^2 q_0}\frac{1}{\xi_M q_0}\frac{d\lambda}{dk^2}\int_0^{\pi} d\theta \times \sqrt{1 - k^2\sin^2\theta} + \frac{1}{k^4 q_0^2 \xi_M^2} - \frac{1}{k^4 q_0^2 \xi_M^2}$$

$$= \frac{d\lambda}{dk^2}\frac{2}{\lambda^2 q_0}\left(\pi - \frac{1}{k\xi_M q_0}\int_0^{\pi} d\theta\sqrt{1 - k^2\sin^2\theta}\right) \quad [32]$$

The desired equation for determining k as a function of H is obtained by setting $dg/dk^2 = 0$:

$$\xi_M q_0 = \sqrt{\frac{K_{22}}{\Delta\chi}}\frac{\pi}{H\lambda_0} = \frac{2}{\pi}\frac{1}{k}\int_0^{\frac{\pi}{2}} d\theta\sqrt{1 - k^2\sin^2\theta}. \quad [33]$$

Define

$$E_1(k) \equiv \int_0^{\frac{\pi}{2}} \frac{d\theta}{\sqrt{1 - k^2\sin^2\theta}},$$

$$E_2(k) \equiv \int_0^{\frac{\pi}{2}} d\theta\sqrt{1 - k^2\sin^2\theta},$$

where E_1 and E_2 are the complete elliptic integrals of the first kind and the second kind, respectively. Eqs. [29] and [33] can be put in the form

$$\lambda = 2\xi_M k E_1(k),$$

and

$$\frac{\pi\xi_M}{\lambda_0} = \frac{2}{k\pi}E_2(k),$$

Combining the two equations yields

$$\frac{\lambda}{\lambda_0} = \frac{4}{\pi^2}E_1(k)E_2(k). \qquad [34]$$

$E_1(k)$ diverges at $k = 1$. Therefore, λ/λ_0 diverges at a field given by Eq. [33]:

$$\frac{\xi_M\pi}{\lambda_0} = \frac{2}{\pi}E_2(1) = \frac{2}{\pi},$$

which defines a critical magnetic field

$$H_c = \sqrt{\frac{K_{22}}{\Delta\chi}}\frac{\pi^2}{2\lambda_0}. \qquad [35]$$

If one takes $K_{22} \sim 10^{-6}$ dyne, $\Delta\chi \sim 10^{-6}$ cgs units, $\lambda_0 \sim 10^{-4}$ cm, H_c is ~50 kOe. A similar threshold can be obtained if the magnetic field is replaced by an electric field:

$$E_c = \sqrt{\frac{4\pi K_{22}}{\Delta\epsilon}}\frac{\pi^2}{2\lambda_0}. \qquad [36]$$

Eqs. [29], [33], [34], and [35] were first obtained by de Gennes.[12] In terms of H_c, Eq. [33] can be put in the form

$$\frac{H_c}{H}k = E_2(k). \qquad [33a]$$

For $H > H_c$ this equation has no solution. When $H < H_c$, the values of k ranges from 0 to 1 as plotted in Fig. 12. In Fig. 13 we show a plot of λ/λ_0 vs. H/H_c. At $H = H_c$ the pitch diverges and the cholesteric phase transforms into the nematic phase. Experimentally this curve is well verified.[13,14]

Finally, it should be noted that if the field is initially applied parallel to the helical axis, the cholesteric helix would usually rotate at $H < H_c$ so as to make the field perpendicular to the helical axis. Therefore, the geometry shown in Fig. 10 is always the situation seen experimentally just before the field strength reaches the cholesteric–nematic transition threshold.[14]

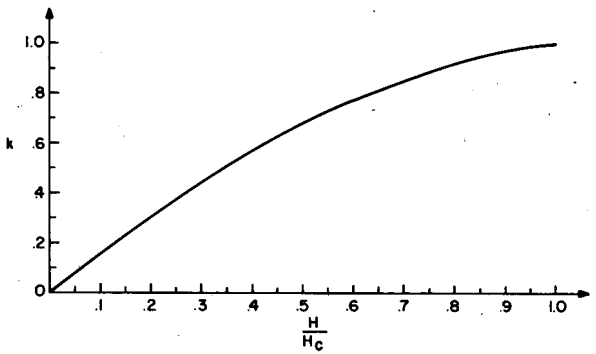

Fig. 12—Solution of Eq. [33a].

4. Concluding Remarks

The above discussion of the continuum theory of liquid crystals is by no means complete. There exist many more effects that can be described by the continuum theory, either in its present or modified form. In view of the diverse applications of the theory, the selection

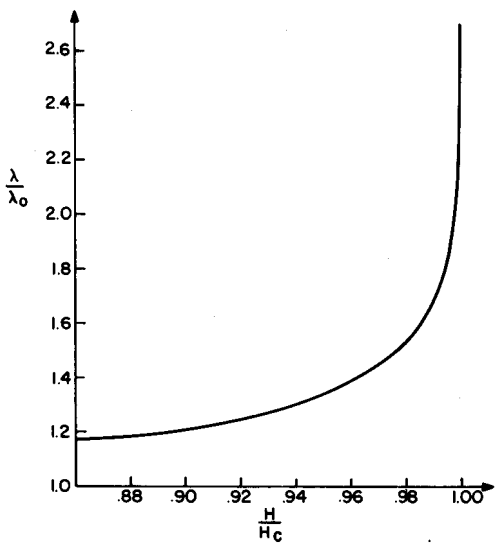

Fig. 13—Ratio of the helical pitch in finite field to the pitch in zero field, λ/λ_0, plotted as a function of reduced field H/H_c. The divergence at $H/H_c = 1$ is logarithmic in nature.

of the four examples discussed in this chapter is based on the consideration that they all have practical relevance to liquid-crystal display devices. It is hoped that their description by the continuum theory can, on the one hand, demonstrate the power and the flavor of the theory and, on the other hand, complement the discussion of the device physics aspects of these effects in other papers of this series.

Appendix

In this appendix we show the steps leading from Eq. [30] to Eq. [31]. From Eqs. [28a] and [30] we have

$$g = \frac{1}{\lambda}\int_0^{\pi} d\theta \frac{k\xi_M}{\sqrt{1 - k^2\sin^2\theta}} \left\{1 - \frac{2\sqrt{1 - k^2\sin^2\theta}}{kq_0\xi_M} + \frac{1 - k^2\sin^2\theta}{k^2q_0^2\xi_M^2} - \frac{\sin^2\theta}{q_0^2\xi_M^2}\right\}$$

$$= \frac{k\xi_M}{\lambda}\int_0^{\pi} d\theta \frac{d\theta}{\sqrt{1 - k^2\sin^2\theta}} - \frac{2\pi}{\lambda q_0} + \frac{1}{k\lambda\xi_M q_0^2}$$

$$\times \int_0^{\pi} d\theta \sqrt{1 - k^2\sin^2\theta} - \frac{1}{q_0^2\lambda\xi_M^2}\int_0^{\lambda} dx \sin^2\theta. \qquad [37]$$

By writing $\sin^2\theta = (1/k^2) - \xi_M^2(d\theta/dx)^2$, the fourth term in Eq. [37] can be simplified as

$$-\frac{1}{q_0^2\lambda\xi_M^2}\int_0^{\lambda} dx \sin^2\theta = -\frac{1}{k^2q_0^2\xi_M^2} + \frac{1}{q_0^2\lambda}\int_0^{\pi}\left(\frac{d\theta}{dx}\right)d\theta$$

$$= -\frac{1}{k^2q_0^2\xi_M^2} + \frac{1}{k\lambda\xi_M q_0^2}\int_0^{\pi} d\theta\sqrt{1 - k^2\sin^2\theta} \qquad [38]$$

Therefore,

$$g = 1 - \frac{2\pi}{\lambda q_0} + \frac{2}{k\lambda\xi_M q_0^2}\int_0^{\pi} d\theta\sqrt{1 - k^2\sin^2\theta} - \frac{1}{k^2q_0^2\xi_M^2}. \qquad [39]$$

References

[1] P. J. Wojtowicz, "Introduction to the Molecular Theory of Nematic Liquid Crystals," Chapter 3.
[2] P. J. Wojtowicz, "Generalized Mean Field Theory of Nematic Liquid Crystals," Chapter 4.
[3] H. Zocher, "The Effect of a Magnetic Field on the Nematic State," *Trans. Faraday Soc.*, **29**, p. 945 (1933).

[4] C. W. Oseen, "The Theory of Liquid Crystals," *Trans. Faraday Soc.*, **29**, p. 883 (1933).

[5] F. C. Frank, "On the Theory of Liquid Crystals," *Faraday Soc. Disc.*, **25**, p. 19 (1958).

[6] E. G. Priestley, "Nematic Order: The Long Range Orientational Distribution Function," Chapter 6.

[7] P. Sheng, "Hard Rod Model of the Nematic-Isotropic Phase Transition, Chapter 5.

[8] P. G. de Gennes, *Lecture Notes on Liquid Crystal Physics*, Part I (1970).

[9] A. Saupe, "Temperaturabhängigkeit und Grösse der Deformationskonstanten nematischer Flüssigkeiten," *Z. Naturforsch.*, **15a**, 810 (1960).

[10] V. Fréedericksz and A. Repiewa, "Theoretisches und Experimentelles zur Frage nach der Natur der Anisotropen Flussigkeiten," *Z. Physik*, **42**, p. 532 (1927).

[11] V. Fréedericksz and V. Zolina, "Forces Causing the Orientation of an Anisotropic Liquid," *Trans. Faraday Soc.*, **29**, p. 919 (1933).

[12] P. G. de Gennes, "Calcul de la Distorsion d'une Structure Chlosteric par un Champ Magnetique," *Solid State Comm.*, **6**, p. 163 (1968).

[13] G. Durand, L. Leger, F. Rondelez, and M. Veyssie, "Magnetically Induced Cholesteric-to-Nematic Phase Transition in Liquid Crystals," *Phys. Rev. Lett.*, **22**, p. 227 (1969).

[14] R. B. Meyer, "Distortion of a Cholesteric Structure by a Magnetic Field," *Appl. Phys. Lett.*, **14**, p. 208 (1969).